12th International Conference on Applications of Statistics and Probability in Civil Engineering, ICASP12
Vancouver, Canada, July 12-15, 2015

Probabilistic Hazard Model of Inelastic Oscillator based on Semi-theoretical Solutions of First Passage Problem

Yasuhiro Mori
Professor, Grad. School of Environmental Studies, Nagoya Univ., Nagoya, Japan

Masato Takashima
Grad. Student, Grad. School of Environmental Studies, Nagoya Univ., Nagoya, Japan

Sayo Kojima,
Kozo Keikaku Engineering, Inc., Tokyo Japan

Fuminobu Ozaki
Assoc. Professor, Grad. School of Environmental Studies, Nagoya Univ., Nagoya, Japan

ABSTRACT: In this study, an approximate method of estimating the exceedance probability of the maximum ductility factor of an inelastic oscillator is proposed based on the equivalent linearization technique using the capacity spectrum (CS) method. The CS method seeks to determine the first point at which the demand spectrum crosses the CS. Because the auto-correlation function of the response spectrum is only a function of the difference between the logarithms of two natural periods, the CS method can be interpreted as the first passage problem of a stationary standard normal stochastic process. Because the auto-correlation function is not continuous when the difference is equal to zero, and because the crossing event cannot be modeled as a Poisson process when the CS is close to the horizontal axis, the mean crossing rate is semi-theoretically estimated based on Monte Carlo simulation. The results are further modified to create a general model. The accuracy of the proposed method is demonstrated by using numerical examples.

1. INTRODUCTION

Predictors of seismic structural demands (such as interstory drift ratios) that are faster than nonlinear dynamic analysis (NDA) are useful for structural performance assessment and design. Several techniques for realizing such predictors have been proposed by using the results of a nonlinear static pushover analysis (e.g., Luco 2002; Chopra & Goel 2002; Yamanaka et al. 2003; Mori et al. 2006). These techniques often use the maximum response of an inelastic oscillator (computed via NDA) that is equivalent to the original frame.

In reliability-based seismic design of a structure, it is necessary to probabilistically express the maximum response of the inelastic oscillator. This information can be obtained via NDA, but requires thousands of samples. In practice, the use of simpler methods, such as an equivalent linearization technique (EqLT), using an elastic response spectrum seems more reasonable; design spectra are being developed on the basis of probabilistic approaches such as uniform hazard spectrum (UHS) and conditional mean spectrum (CMS, Baker & Jayaram 2008).

A UHS is obtained by plotting the response with the same (i.e., uniform) exceedance probability for a suite of elastic oscillators with different natural periods; hence, a UHS represent no specific ground motion (Abrahamson 2006). Although there exists certain correlation among the spectral responses of elastic oscillators to a ground motion (e.g., Baker

& Jayaram 2008), perfect correlation is implicitly assumed in the use of a UHS. In such a scenario, the response may be overestimated via EqLT when a very rare event is considered.

The correlation among spectral responses may be considered by using a CMS, which is the mean spectrum conditional to the event that the spectral displacement of an elastic oscillator with a certain period equals the displacement with, for example, 10% exceedance probability in 50 years. However, the authors have shown that the EqLT using CMS can provide fairly optimistic estimates (Mori et al 2011).

A new approximation method is proposed using semi-theoretical solutions of the first passage problem by converting a probabilistic elastic displacement response spectrum into a stationary standard normal random process. The accuracy and applicability of the method are discussed by using numerical examples.

2. Equivalent Linearization Techniques

2.1. Equivalent Linearization Technique

In an EqLT, the maximum displacement of an inelastic oscillator with the elastic natural period, T_1, and the damping factor, h_1, is approximated by using the maximum displacement of an elastic oscillator with the equivalent natural period, T_{eq}, and the equivalent damping factor, h_{eq}, as

$$S_D^I(T_1;h_1) \approx S_D^E(T_{eq};h_{eq}) \tag{1}$$

where $S_D(T;h)$ is the spectral displacement of an oscillator with the natural period, T , and the damping factor, h; the superscripts E and I represent the elastic and inelastic responses, respectively. OFten, T_{eq} and h_{eq} are expressed as functions of the maximum ductility factor of the inelastic oscillator, μ, which is defined as

$$\mu = S_D^I(T_1;h_1)/\delta_y \tag{2}$$

where δ_y is the yield displacement of the oscillator. Several linearization techniques have been proposed (e.g., Iwan 1980, Shimazaki 1999); among them, the following formulae proposed by Shimazaki for an oscillator with a bilinear backbone curve are used in this study.

$$T_{eq} = T_1 \cdot \sqrt{\frac{\mu}{1-k_2(1-\mu)}} \tag{3}$$

$$h_{eq} = 0.25 \cdot (1 - 1/\sqrt{\mu}) + h_1 \tag{4}$$

where k_2 is the second stiffness ratio of the backbone curve.

2.2. Capacity Spectrum Method

The capacity spectrum (CS) method (Freeman 1978) can be used to graphically estimate the inelastic displacement as the intersection of the capacity spectrum and the demand spectrum (DS). To take into account the effect of h_{eq}, the demand spectrum must be adjusted by multiplying it with the damping reduction factor, $F_h(h_{eq})$, defined as the ratio of the spectral response of an elastic oscillator with a damping factor to that with the damping factor, h_1. Because h_{eq} is a function of the unknown value μ, an iterative procedure is generally required for its determination.

In contrast, the response can be estimated directly by considering the demand and capacity spectra in an ordinal T-S_D coordinate rather than an S_D-S_A coordinate, as shown in Fig.1 (Mori & Maruyama 2007). The S_D axis can be transformed linearly into the axis of the maximum ductility factor, μ, by dividing the S_D axis by the yield displacement of the inelastic oscillator. The T axis can also be expressed in terms of μ because T_{eq} is a function of μ, as expressed by Eq.(3). Then, the capacity spectrum can be obtained by connecting the corresponding values in the linear (vertical) and nonlinear (horizontal) μ coordinates.

On the basis of Eq.(3), the capacity spectrum, $C_S(T)$, of an inelastic oscillator with a bilinear backbone curve and mass equal to unity can be expressed as,

$$\begin{aligned} C_S(T) &= \delta_y \cdot \mu \\ &= \frac{9.8 \cdot C_y}{k_1} \cdot \frac{(1-k_2) \cdot T^2}{T_1^2 - k_2 \cdot T^2} \\ &= \frac{9.8 \cdot C_y \cdot T_1^2}{4\pi^2} \cdot \frac{(1-k_2) \cdot T^2}{T_1^2 - k_2 \cdot T^2} \; ; \; T \geq T_1 \end{aligned} \tag{5}$$

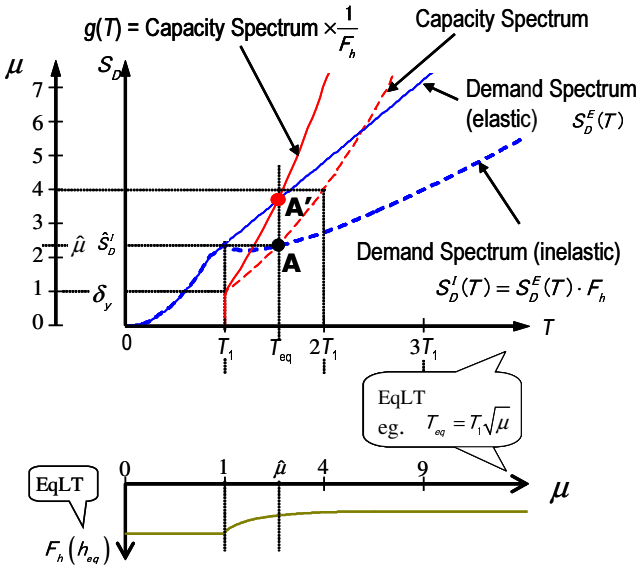

Figure 1: Capacity-Spectrum Method in T-S_D Coordinate)

where k_1 and C_y are the elastic stiffness and yield base shear coefficient of the oscillator, respectively; the acceleration attributable to gravity is 9.8 (m/s^2).

The following damping reduction factor (Kasai et al 2003) is used in this research:

$$F_h(h) = \begin{cases} (D(h)-1)\cdot(5\cdot T)+1 & ;\ 0 \le T \le 0.2 \\ D(h) & ;\ 0.2 \le T \le 2 \\ D(h)\cdot\left[\sqrt{h/h_1}\cdot(T-2)/40+1\right] & ;\ 2 \le T \le 8 \end{cases} \tag{6}$$

where

$$D(h) = \sqrt{\frac{1+25\cdot h_1}{1+25\cdot h}} \tag{7}$$

When the probability distribution and auto-correlation function of the n-year maximum $S_D^E(T;h)$ are available, the exceedance probability of the n-year maximum displacement response of an inelastic oscillator can be estimated by Monte Carlo simulation. This simulation finds the intersection of each sample of $S_D^E(T;h)$, which is a demand spectrum and $C_S(T)/F_h(h_{eq})$, which is hereafter designated a factored CS, $g(T)$, (see Fig.1). However, such a procedure requires extensive computational effort, and thus, a more practical method is investigated in the next section.

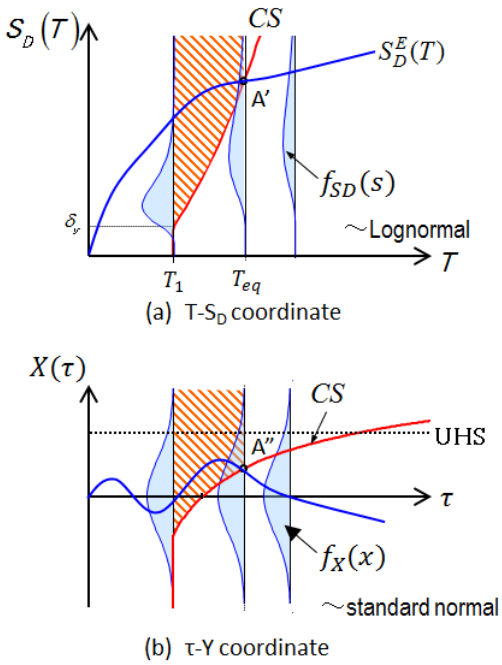

Figure 2: Schematic Illustration of CS and DS in Standard Normal Stochastic Process

3. CS Method as First Passage Problem In Standard Normal Stochastic Process

In the CS method, the event that the equivalent natural period, T_{eq}, is longer than t_{eq} corresponds to the event that $S_D^E(T;h)$ is always above the factored CS in the range of (T_1, t_{eq}) (the hatched area in Fig.2(a)).

According to previous studies such as those by Baker & Jayaram (2008), the auto-correlation function of $S_D^E(T;h)$ is dependent only on the difference between the logarithms of two natural periods as shown in Eq.(8) and Fig.3 (Baker & Jayaram 2008).

$$K_{S_D}(\zeta) = 1 - \cos\left(\frac{\pi}{2} - 0.366\cdot\ln(10)\cdot|\zeta|\right) \tag{8}$$
$$(\zeta = \log(T) - \log(T_1), \quad T_1 \ge 0.109(\mathrm{s}))$$

Therefore, $S_D^E(T;h)$ can easily be transformed into a stationary standard normal stochastic process, $X(\tau)$ where $\tau = \log(T)+1$. Then, the CS method can be interpreted as the first passage problem of a stationary standard normal stochastic process crossing a factored CS, which is accordingly transformed, downward as shown in Fig.2(b)(Mori et al 2011). By this transformation, the DS is normalized and the information regarding structural

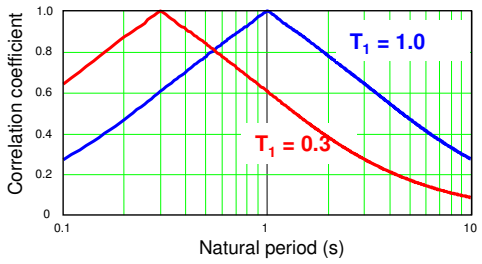

Figure 3: Auto-correlation Model of $S_D^E(T;h)$

characteristics and seismic hazard, except for the auto-correlation function of $S_D^E(T;h)$, is reflected to the shape and position of the factored CS.

When $S_D^E(T,h)$ is lognormally distributed, it can be transformed into a stationary standard normal stochastic process by

$$X(\tau) = \frac{\ln(S_D^E(\tau,h)) - \mu_{\ln(S_D^E(\tau))}}{\sigma_{\ln(S_D^E(\tau))}} \tag{9}$$

in which $\mu_{\ln(S_D^E(\tau))}$ and $\sigma_{\ln(S_D^E(\tau))}$ are the mean and standard deviation of $\ln(S_D^E(\tau))$, respectively.

4. First Passage Problem of Stationary Standard Stochastic Process

4.1. Theoretical Solution of Mean Crossing Rate

Consider an event that a stationary standard normal stochastic process, $X(\tau)$, crosses a constant threshold a downward. The mean crossing rate, ν_a, can be expressed by

$$\nu_a = \frac{\sigma_V}{\sqrt{2\pi}}\phi(a) \tag{10}$$

in which $\phi(\bullet)$ is the standard normal probability density function, and σ_V is the standard deviation of $V(\tau) = dX(\tau)/d\tau$, which can be expressed as

$$\sigma_V = \sqrt{-\frac{d^2K_X(\zeta)}{d\zeta^2}\bigg|_{\zeta=0}} \tag{11}$$

in which $K_X(\zeta)$ is the auto-correlation function of $X(\tau)$, which depends only on the time difference, $\zeta = \tau_1 - \tau_2$.

If the events of crossing a threshold a are rare, the occurrence of the events can be modeled by a Poisson process, and the probability, $P_0(t_L)$, that no crossing occurs within time interval $(0,t_L)$ can be approximately expressed as,

$$\begin{aligned} P_0(\tau_L) &= P[X(\tau) > a; 0 < \tau < \tau_L] \\ &= \exp(-\nu_a \cdot \tau_L) \end{aligned} \tag{12}$$

If the threshold varies with time, the mean crossing rate can be expressed as,

$$\nu_a(\tau) = \left[A - \dot{a}\left\{1 - \Phi\left(\frac{\dot{a}}{\sigma_V}\right)\right\}\right] \cdot \phi\{a(\tau)\} \tag{13}$$

in which $\dot{a} = da(\tau)/d\tau$, $\Phi(\bullet)$ is the standard normal probability distribution function, and

$$A = \frac{\sigma_V}{\sqrt{2\pi}} \exp\left\{-\frac{1}{2}\left(\frac{\dot{a}}{\sigma_V}\right)^2\right\} \tag{14}$$

Similar to Eq.(12), if the events of crossing threshold $a(\tau)$ are rare, the occurrence of these events can also be modeled by a nonstationary Poisson process, and the probability, $P_0(\tau_L)$, that no crossing occurs within time interval $(0,\tau_L)$ can be approximately expressed as

$$P_0(\tau_L) = \exp\left(-\int_0^{\tau_L} \nu_a(\tau)d\tau\right) \tag{15}$$

4.2. Mean Crossing Rate Based on Simulation

To estimate a mean crossing rate by using Eqs.(12) or (15), the second-order derivative of the auto-correlation function of $X(\tau)$ must be available at $\zeta = 0$, as shown in Eq.(11). However, as shown in Eq.(8) and Fig.3, the auto-correlation function of $S_D^E(T;h)$ is not continuous at $\zeta = 0$; accordingly, it is not differentiable.

Even if a mean crossing rate can be estimated accurately, the exceedance probability cannot be accurately estimated by using Eqs.(12) or (15) if the threshold is close to the horizontal axis. Under such circumstances, the crossing event would not be rare and cannot be modeled by a Poisson process.

In this research, attempts are made to estimate σ_V in Eq.(10) based on Monte Carlo simulation so that the exceedance probability can be estimated by using Eqs.(12) or (15).

The auto-correlation function expressed by Eq.(8) is affected by the nonlinear transformation of $S_D^E(T;h)$ into a standard normal stochastic process. If $S_D^E(T;h)$ is lognormally distributed, the

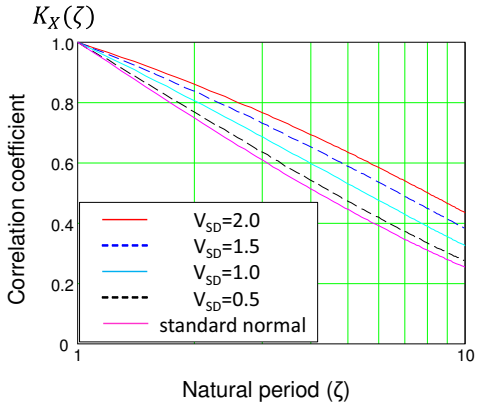

Figure 4: Auto-correlation Model of $S_D^E(T;h)$

auto-correlation function of $X(\tau)$ can be expressed as (Der Kiureghian and Liu 1985)

$$K_X(\zeta) = \frac{\ln\left(1+K_S(\zeta)\cdot V_{S_D(T_1)}\cdot V_{S_D(T)}\right)}{\sqrt{\ln\left(1+V^2_{S_D(T)}\right)}\cdot\sqrt{\ln\left(1+V^2_{S_D(T)}\right)}} \quad (16)$$

in which $V_{S_D(T)}$ and $K_S(\zeta)$ are the coefficient of variation (c.o.v.) and the auto-correlation function of $S_D^E(T;h)$, respectively. Fig.4 illustrates examples of $K_X(\zeta)$ when $S_D^E(T;h)$ is lognormally distributed with constant c.o.v. equal to 0.5, 1.0, 1.5, or 2.0 along with that expressed by Eq.(8).

4.2.1. σ_V for Crossing Constant Threshold

σ_V is determined iteratively for each constant threshold within the range of $a=-3$ to 2.5 by Monte Carlo simulation with 40,000 samples so that the exceedance probability estimated by the simulation agrees with that estimated by Eqs.(10)-(12). Fig.5 shows examples of agreement and non-agreement. The increment of τ in the simulation is set to be 0.01.

During the course of research, it was found that a constant value of σ_V cannot provide an accurate estimate of the exceedance probability, particularly when a is large (see Fig.5(b)). Thus, σ_V is modeled here as a function of τ, expressed by Eqs.(17)-(19).

$$\sigma_V(a,\tau,dK) = \sigma_{V0}(a)\cdot\{1-f(\tau)\cdot g(a,dK)\} \quad (17)$$

in which

$$f(\tau) = 0.68\cdot\Phi\left(\frac{\ln(\tau)-\ln(0.06)}{0.5}\right) \quad (18)$$

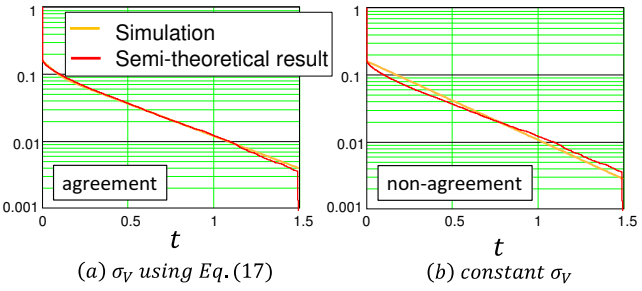

Figure 5: Example of Satisfactory Agreement and Non-agreement of Exceedance Probability between Simulation and Semi-theoretical Result ($a=1$)

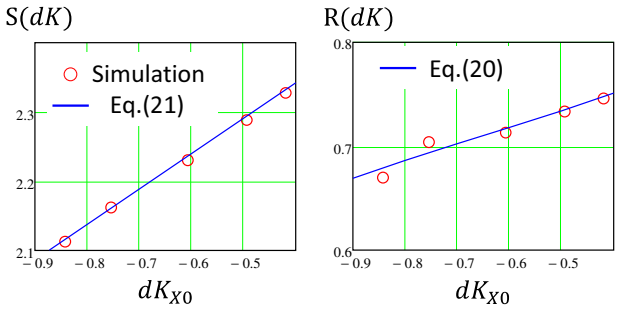

Figure 6: $S(dK)$and$R(dK)$ Estimated by Simulation

$$g(a,dK) = \begin{cases} 1-\Phi\left(\dfrac{\sqrt{-a}-R(dK)}{S(dK)}\right) & (a<0) \\ 1 & (a\geq 0) \end{cases} \quad (19)$$

$f(\tau)$ in Eq.(17) considers that σ_V depends on τ, and $g(a,dK)$ in the equation considers that the dependency of σ_V on τ depends on threshold level a. In Eq.(19), $R(dK)$ and $S(dK)$ are determined iteratively, as shown in Fig.6 and modelled by a linear function of $dK=(K_X(0.01)-K_X(0))/0.01$ as

$$R(dK) = 0.503\cdot dK + 2.54 \quad (20)$$
$$S(dK) = 0.162\cdot dK + 0.815 \quad (21)$$

Then, $\sigma_{V0}(a)$ in Eq.(17) is determined for each threshold based on the simulation.By expressing the horizontal axis with $\log\{1-\Phi(a)\}$ and the vertical axis with $\log\{\sigma_{V0}(a)\}$, $\sigma_{V0}(a)$ is intriguingly plotted on a straight line as shown in Fig.7. Accordingly, $\sigma_{V0}(a)$ is modeled as

$$\sigma_{V0}(a) = 10^{\{k(dK)-1.034\cdot\log(1-\Phi(a))\}} \quad (22)$$

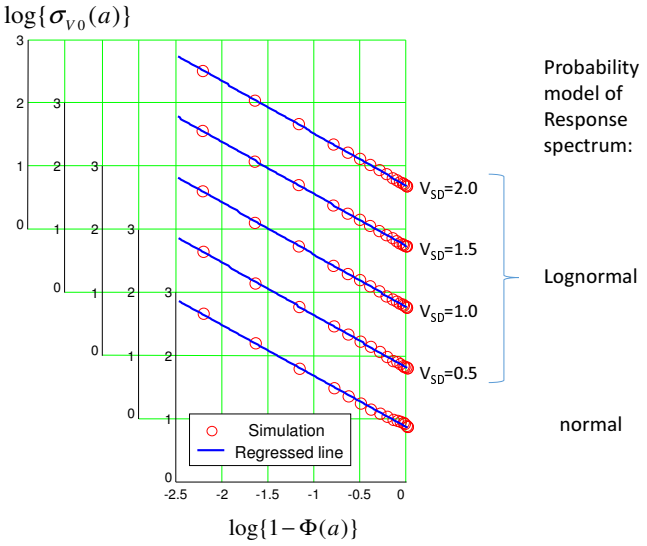

Figure 7: σ_{V0} Estimated by Simulation

in which

$$k(dK) = -0.42 \cdot dK + 0.686 \tag{23}$$

4.2.2. σ_V for Crossing Time-varying Threshold

When the threshold varies with time, further modification on the mean crossing rate is necessary. Based on the iterative analysis, the mean crossing rate is determined considering the instantaneous slope of the threshold, $\dot{a}$, as

$$\nu_a(\tau,\dot{a}) = \nu_a(\tau) \cdot \left(1 + \dot{a} \cdot \frac{1}{h(dK,\tau)}\right) \tag{24}$$

in which $\nu_a(\tau$ is estimated by using Eq.(13) with σ_V estimated by Eqs.(10)-(12), and

$$\begin{aligned} h(dK,\tau) &= f_1(dK,\tau) \\ &\cdot(1 + f_2(dK,\tau) \cdot g_1(\tau) \cdot g_2(dK,\tau)) \end{aligned} \tag{25}$$

where

$$g_1(\tau) = \begin{cases} -0.68 \cdot \Phi\left(\dfrac{\tau}{0.5}\right) & ;\dot{a} \le 0 \\ -0.68 \cdot \Phi\left(\dfrac{\tau - 0.1 \cdot \dot{a}}{0.5}\right) & ;\dot{a} > 0 \end{cases} \tag{26}$$

$$g_2(dK,\tau) = \begin{cases} 1 - \Phi\left(\dfrac{\sqrt{a(\tau)} - (0.503 \cdot dK + 2.54)}{0.162 \cdot dK + 0.815}\right) & ;a(\tau) \le 0 \\ 1 & ;a(\tau) > 0 \end{cases} \tag{27}$$

$$f_1(dK,\tau) = \begin{cases} f_{11} - 1.5 \cdot f_{12} & ;\dot{a} \le -1.5 \\ f_{11} + \dot{a} \cdot f_{12} & ;\dot{a} > -1.5 \end{cases} \tag{28}$$

$$\begin{aligned} f_{11} &= 0.56 - 0.125 \cdot dK \\ &\quad + a(0) \cdot (-0.139 - 0.054 \cdot dK) \end{aligned} \tag{29}$$

$$\begin{aligned} f_{12} &= 0.493 + 0.384 \cdot dK \\ &\quad + a(0) \cdot (-0.096 - 0.078 \cdot dK) \end{aligned} \tag{30}$$

$$f_2(dK,\tau) = \begin{cases} f_{21} + \dot{a} \cdot f_{22} & ;\dot{a} \le 0.5 \\ f_{21} + 0.5 \cdot f_{22} & ;\dot{a} > 0.5 \end{cases} \tag{31}$$

$$\begin{aligned} f_{21} &= 0.832 + 0.018 \cdot dK \\ &\quad + a(0) \cdot (-0.06 - 0.009 \cdot dK) \end{aligned} \tag{32}$$

$$\begin{aligned} f_{22} &= -0.489 - 0.276 \cdot dK \\ &\quad + a(0) \cdot (-0.008 - 0.032 \cdot dK) \end{aligned} \tag{33}$$

5. Numerical Examples

Fig.8 shows the maximum ductility factor of inelastic oscillators with elasto-plastic backbone curves. It is assumed that the oscillator is subjected to a seismic hazard with the following characteristics:

- $S_D^E(T;h)$ is lognormally distributed, with autocorrelation function given by Eq.(8). The case when $S_D^E(T;h)$ is normally distributed is also considered, simply for reference.
- The 90% non-exceedance probability of the response spectrum is given by the design spectrum prescribed in the Japanese seismic provisions as shown in Fig.9. The characteristic period of the response spectrum, T_g, defined as the boundary between the acceleration constant domain and the velocity constant range, is equal to 0.86 s.
- The c.o.v. of $S_D^E(T;h)$, which is lognormally distributed, is constant for any value of the natural period and equal to 0.5, 1.0, 1.5, or 2.0. When $S_D^E(T;h)$ is normally distributed, the c.o.v. is constant and equal to 0.5.

The following characteristics of the oscillator are considered:

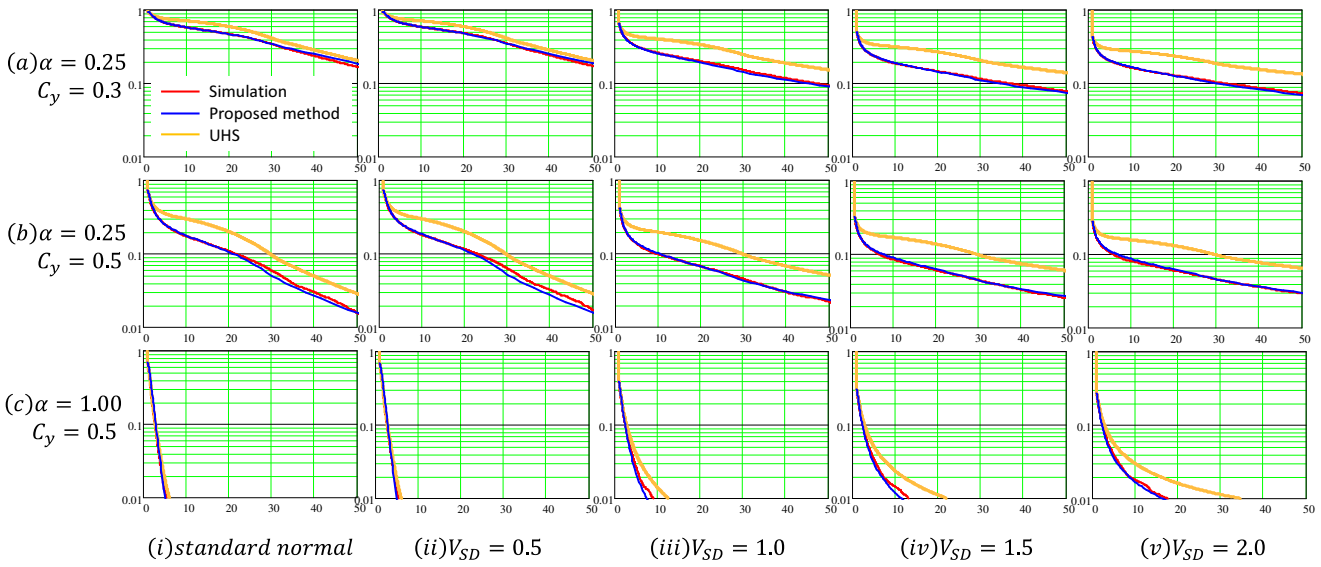

Figure 8: Exceedance probability of maximum ductility factor

- Yield base shear, C_y =0.3 or 0.5.
- Natural period, $T_1 = \alpha \cdot T_g$ with α =0.25, 0.5, or 1.0.
- Damping factor, h=0.05

The CS transformed into the standard normal stochastic process is illustrated in Fig.10.

In Fig.8, the maximum ductility factors estimated by Monte Carlo simulation as rigorous estimates, and those by EqLT using UHS, are presented by red and yellow lines, respectively. As shown in the figure that EqLT using UHS provides an erroneous estimate, particularly when the c.o.v. of the C_y is large and α is small. On the contrary, the proposed method provides a fairly accurate estimate in most cases.

6. CONCLUSIONS

In this study, an approximate method of estimating the exceedance probability of the maximum ductility factor of an inelastic oscillator is proposed based on the equivalent linearization technique using a capacity spectrum (CS) method. The CS method seeks to determine the first point at which demand spectrum (DS) crosses the CS. Because the auto-correlation function of response spectrum is only a function of the difference between the logarithms of two natural periods, the response spectrum, which is DS in the CS method, can easily

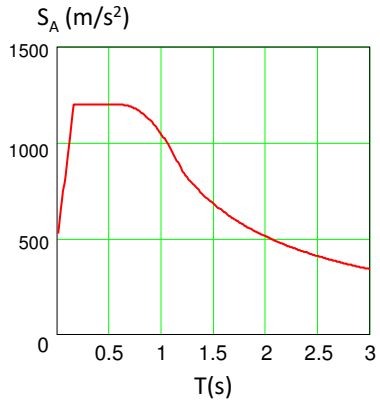

Figure 9: Design Spectrum in Japanese Seismic Provision

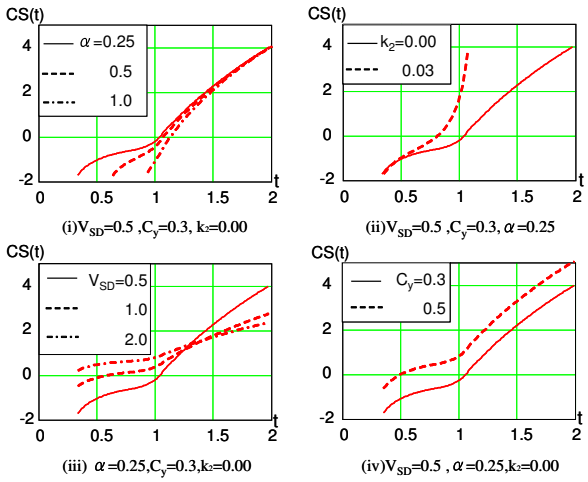

Figure 10: CS in Standard Normal Stochastic Process

be transformed into a stationary standard normal stochastic process. Thus, the CS method can be in-

terpreted as a first passage problem of a stationary standard normal stochastic process. Because the auto-correlation function is not continuous when the difference is equal to zero, and because the crossing event cannot be modeled as a Poisson process when CS is close to the horizontal axis, the mean crossing rate is estimated semi-theoretically based on Monte Carlo simulation. The results are further modified to create a general model. The accuracy of the proposed method is demonstrated by using numerical examples.

In this study, only a single spectral displacement is considered. Because the preceding conclusions may be dependent on the shape of the displacement spectrum, further investigation is necessary, along with possible improvement and simplification of the proposed method.

ACKNOWLEDGMENTS

The authors gratefully acknowledge the financial support provided through a Grant-in-Aid for Scientific Research (B) (No.25282100) by the Ministry of Education, Science, Sports, and Culture and the Japan Society for the Promotion of Science.

7. REFERENCES

Abrahamson, N., (2006). "Seismic hazard assessment: problems with current practice and future developments," *Proc. 1st European Conf. on Earthquake Engineering & Seismology*, Geneva, Switzerland, 1-17.

Baker, J.W. and Jayaram, N., (2008). "Correlation of Spectral Acceleration Values from NGA Ground Motion Models." *EarthquakeSpectra*, Vol.24, No.1, pp.299-317.

Chopra, A.K. and R.K. Goel, (2002). "A modal pushover analysis procedure for estimating seismic demands for buildings," *Earthquake Engineering & Structural Dynamics*, 31(3), 561-582.

Freeman, S.A., (1978). "Prediction of response of concrete buildings to severe earthquake motion," *Douglas McHenry Int. Symp. on Concrete and Concrete Structures*, SP-55, ACI, 589-605.

Der Kiureghian, A. and P-L. Liu, (1985). "Structural reliability under incomplete probability information," *J. Engineering Mechanics*, ASCE, 112, 85-104.

Iwan, W.D., (1980). "Estimating inelastic response spectra from elastic spectra," *Earthquake Engineering & Structural Dynamics*, 8, 375-388.

Kasai, K., H. Ito, and A. Watanabe, (2003). "Peak response prediction rule for a SDOF elasto-plastic system based on equivalent linearization technique," *J. Structural & Construction Engineering*, 571, 53-62. (in Japanese)

Luco, N., (2002). *Probabilistic Seismic Demand Analysis, SMRF Connection Fractures, and Near-source Effects*. Ph.D. Dissertation; Stanford University, Stanford, California.

Mori, Y., T. Yamanaka, N. Luco, and C.A. Cornell, (2006). "A static predictor of seismic demand on frames based on a post-elastic deflected shape," *Earthquake Engineering & Structural Dynamics*, 35, 1295-1318.

Mori, Y. and M. Maruyama, (2007). "Seismic structural demands taking accuracy of response estimation into account," *Earthquake Engineering & Structural Dynamics*, 36, 1999-2020.

Mori, Y., Kojima, S., and Ibuki, K., (2011). "Probabilistic Hazard Modelof Inelastic Response of SDOF System Based on EquivalentLinearization Technique," *Application of Probability & Statisticsin Civil Engrg*, 8pp. (CD-ROM).

Shimazaki, K., (1999). "Evaluation of structural coefficient by displacement response estimation using the equivalent linear method," *J. Structural & Construction Engineering*, 516, 51-57. (in Japanese)

Yamanaka, T., Y. Mori, and M. Nakashima, (2003). "Estimation of displacement response of multi-story frame considering modal shape after yielding," *Summaries of Technical Papers of Annual Meeting*, AIJ, B-1, 563-564. (in Japanese)